Molecular Cell, Volume *83*

Supplemental information

Stepwise activities of mSWI/SNF family chromatin remodeling complexes direct T cell activation and exhaustion

Elena Battistello, Kimberlee A. Hixon, Dawn E. Comstock, Clayton K. Collings, Xufeng Chen, Javier Rodriguez Hernaez, Soobeom Lee, Kasey S. Cervantes, Madeline M. Hinkley, Konstantinos Ntatsoulis, Annamaria Cesarano, Kathryn Hockemeyer, W. Nicholas Haining, Matthew T. Witkowski, Jun Qi, Aristotelis Tsirigos, Fabiana Perna, Iannis Aifantis, and Cigall Kadoch

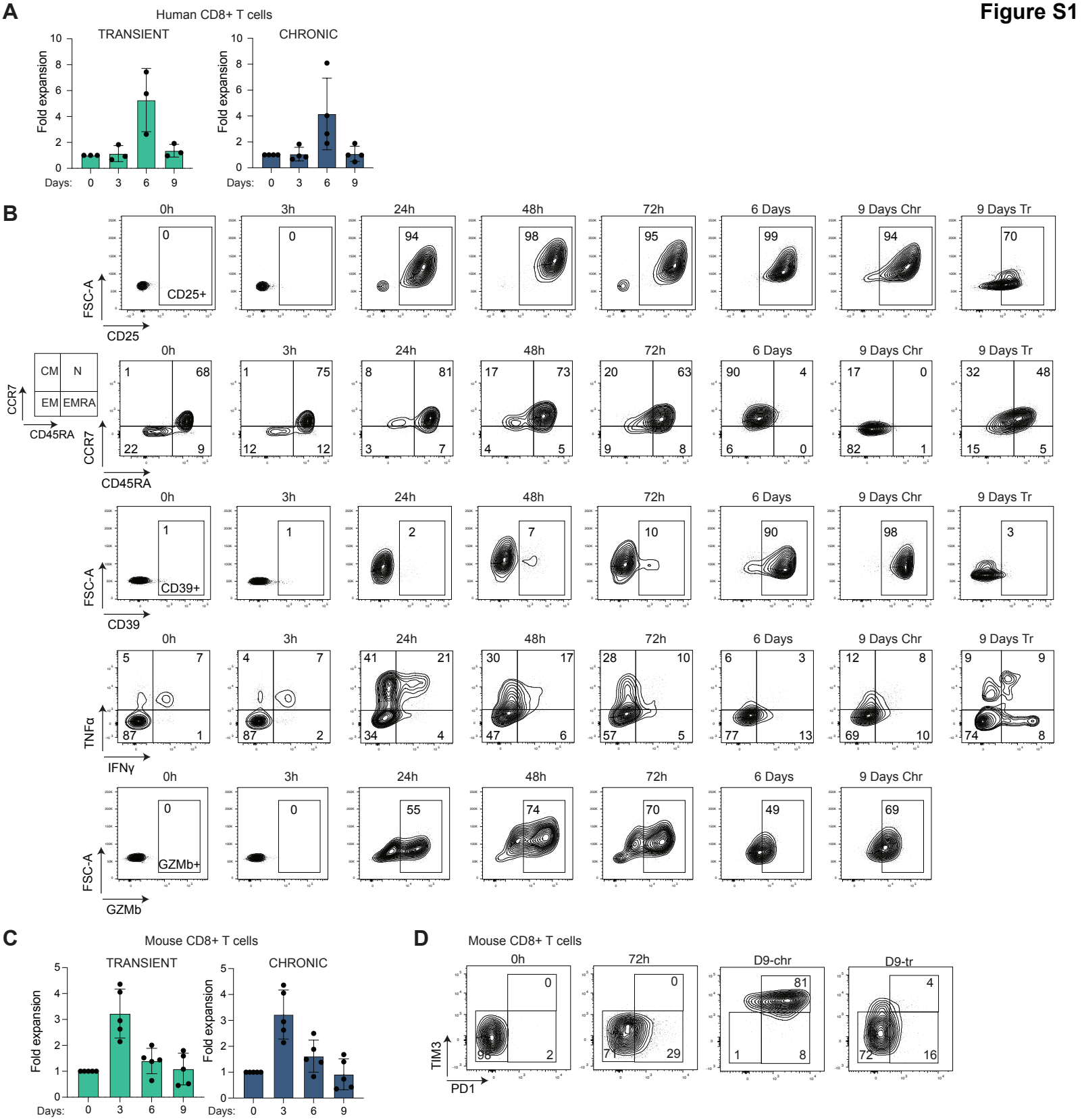

Figure S1. Establishment and characterization of human and mouse CD8+ T cell activation and exhaustion using cell culture systems, Related to Figure 1. A. Fold expansion for human CD8+ T cells in the chronic or transient stimulation conditions across the Day 0, 3, 6, and 9 time points. Bar graphs represent mean ± SEM from 3-4 independent CD8+ T cell donors. **B.** FACS plots depicting the profiling of CD25, CD45RA and CCR7, CD39, IFNγ, TNFα and GZMb across the activation and exhaustion time course. **C.** Fold expansion for mouse CD8+ T cells in the chronic or transient stimulation conditions across the no stim, and Day 3, 6, and 9 time points. Bar graphs represent mean ± SEM from 3-5 independent mice. **D.** FACS-based profiling of PD1 and TIM3 markers indicating putative naïve/memory, activated, and exhausted T cell populations in mouse CD8+ T cell studies.

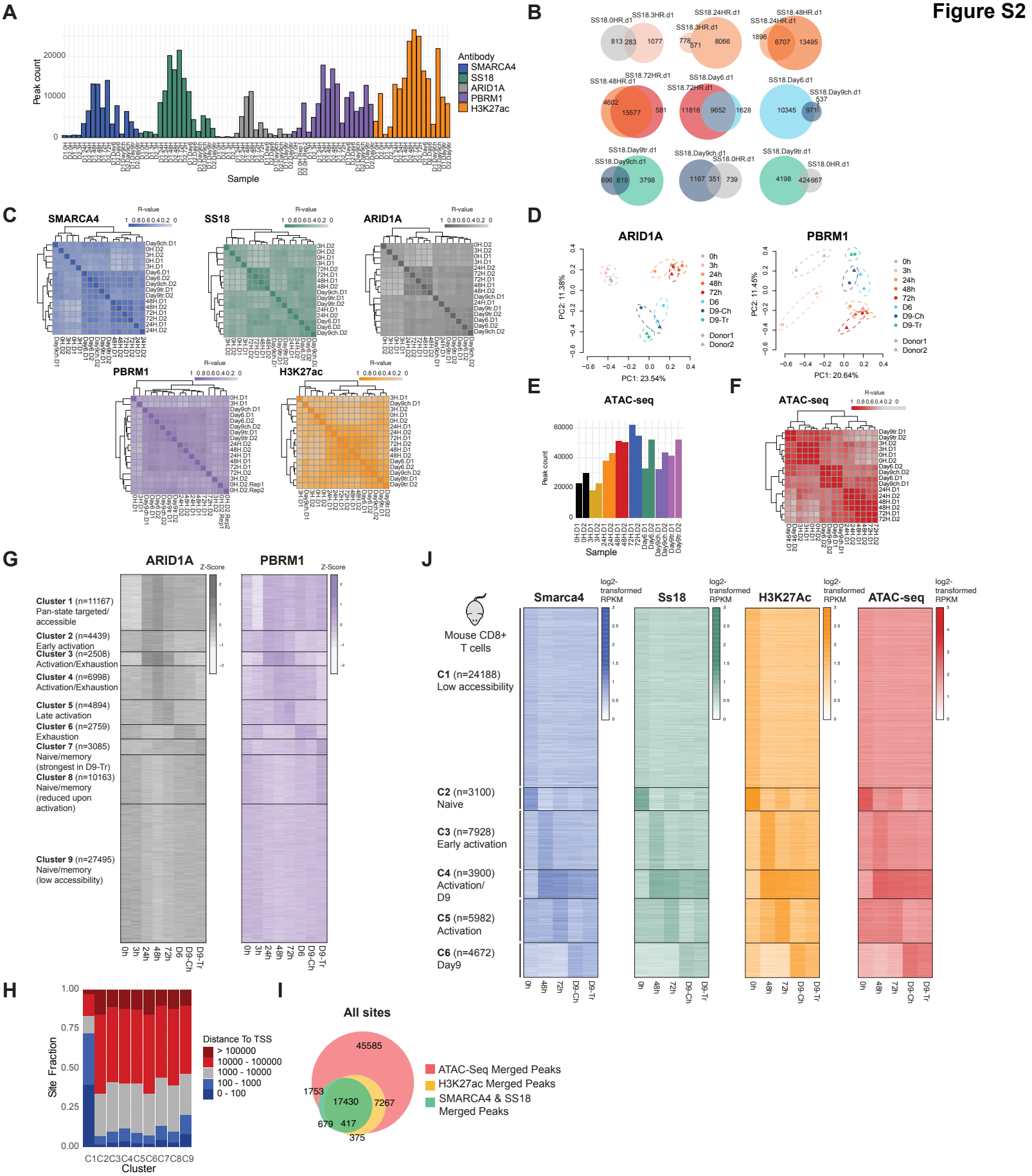

Figure S2. Chromatin occupancy and accessibility profiling of human CD8+ T cells during activation and exhaustion, Related to Figure 1. A. Raw peak counts for SMARCA4, SS18, ARID1A, PBRM1, and H3K27Ac CUT&Tag experiments performed across time course, for 2 independent human donors (denoted as D1,D2). **B.** Venn diagrams reflecting pairwise comparisons of peak numbers for SS18 mSWI/SNF complex subunit CUT&Tag across time points (Donor 1 shown). **C.** Pairwise correlations between all samples for SMARCA4, SS18, ARID1A, PBRM1, and H3K27Ac CUT&Tag occupancy levels within merged peaks. **D.** Principal component analyses (PCA) for ARID1A (cBAF) and PBRM1 (PBAF) CUT&Tag profiles throughout the activation/exhaustion time course. **E.** Peak counts for ATAC-seq experiments performed across time course, for 2 independent human donors. **F.** Pairwise correlations between all samples for ATAC-seq experiments. **G.** K-means clustering for ARID1A and PBRM1 peaks as in Figure 1D; Quantile-normalized Log2-Transformed RPKMs are presented in the heatmap as Z-scores. **H.** Distance-to-TSS plot for Clusters 1-9 from Figure 1D. **I.** Venn diagram reflecting overlap between ATAC-seq accessible peaks, mSWI/SNF complexes (SS18/SMARCA4 merged) and H3K27Ac. **J.** Heatmaps reflecting K-means clustering of quantile-normalized log2-transformed RPKMs from Smarca4, Ss18, H3K27ac, and ATAC-seq merged peaks from mouse CUT&Tag and ATAC-seq experiments.

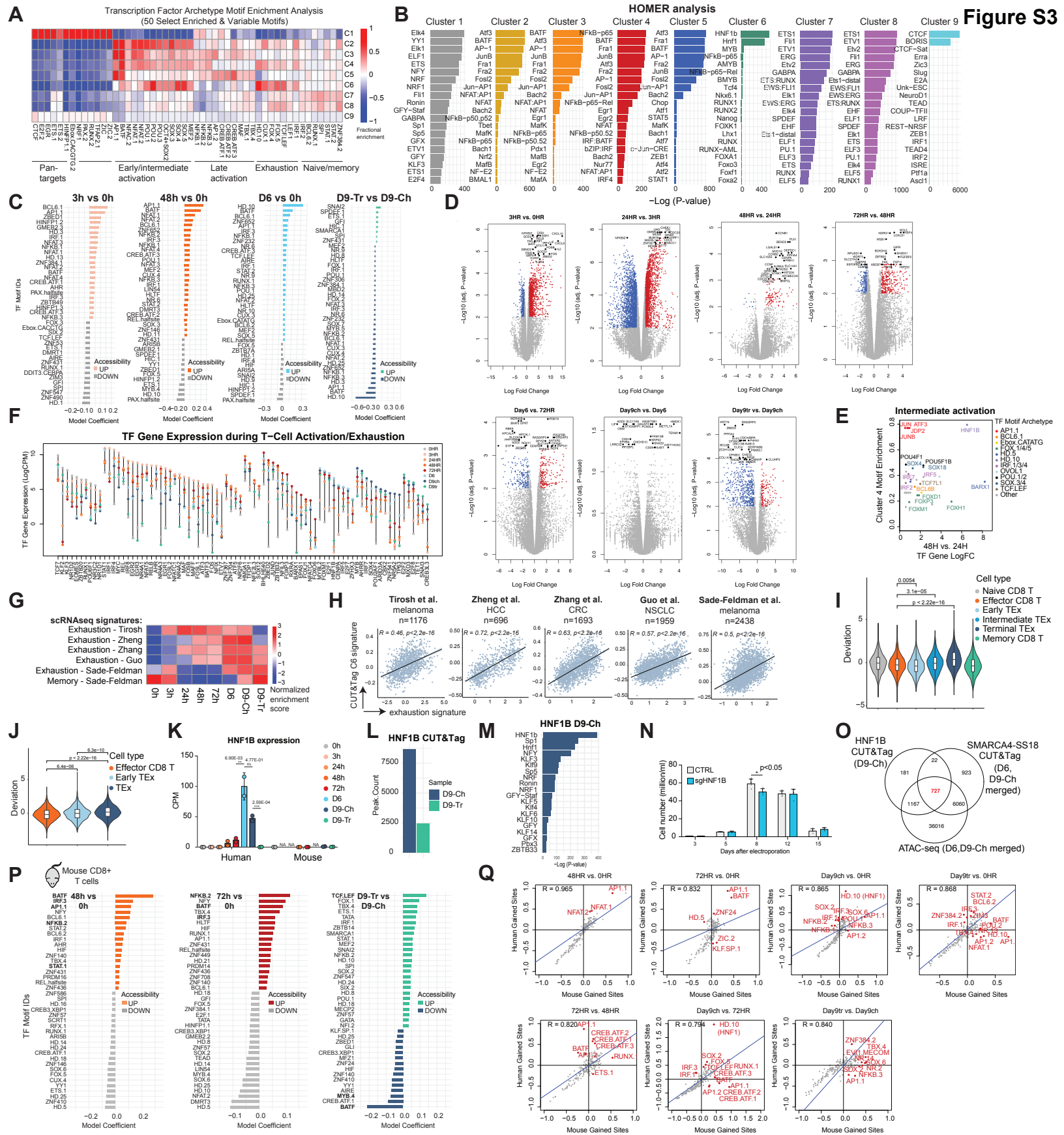

Figure S3. mSWI/SNF targeting and accessibility over TF target genes during human T cell activation and exhaustion, Related to Figure 2,3. A. Fractional motif enrichment in clusters (relative to all sites) for selected archetype motifs with high occurrence and variability. **B.** HOMER motif enrichment analysis across indicated clusters. **C.** Differential motif accessibility between time points indicated (top 40 coefficients of logistic regression models). **D.** Volcano plots of changes in gene expression from n=2 independent donors throughout the time course. Significantly up-regulated and down-regulated genes (Abs Log2FC > 1, FDR < 0.01) are colored in red and blue, respectively. The top 20 differentially expressed genes in every comparison are labeled. **E.** Plot representing state-specific TF fractional motif enrichment (y-axis) and gene expression (x-axis) at the intermediate activation (C4) state. **F.** Gene expression levels (logCPMs) of 80 select TF genes with high expression and variability during T-cell activation and exhaustion. **G.** Enrichment (-log10(p-value)) of mSWI/SNF-bound genes at different time points across signatures derived from scRNAseq datasets. **H.** Correlations between expression changes for genes in C6 (Cluster 6) and exhaustion signatures for each published study. R correlation values and p values are indicated. **I.** HNF1B motif enrichment across cell types in the Satpathy et al. scATAC-seq dataset. **J.** HNF1B motif enrichment across cell types in the Kourtis et al. scATAC-seq dataset. **K.** HNF1B gene expression (CPM) in human and mouse T cells across the activation/exhaustion time course. **L.** HNF1B CUT&Tag raw peak numbers in Day9-Ch and Day9-Tr conditions. **M.** Motif enrichment analysis performed on HNF1B CUT&Tag in Day9-Chr condition. **N.** T cell proliferation in sgCTRL and sgHNF1B conditions. **O.** Venn diagram reflecting overlap between SMARCA4/SS18 CUT&TAG, HNF1B CUT&Tag and ATAC-seq peaks in the Day9-Ch condition. **P.** Top 40 coefficients of logistic regression models fitting motif counts across all sites to changes in accessibility for selected time point comparisons in mouse T-cells during activation and exhaustion. **Q.** Archetype motif fractional enrichment for sites of gained accessibility (LogFC > 0,) relative to all sites in human and mouse settings. Selected motifs are labeled in red.

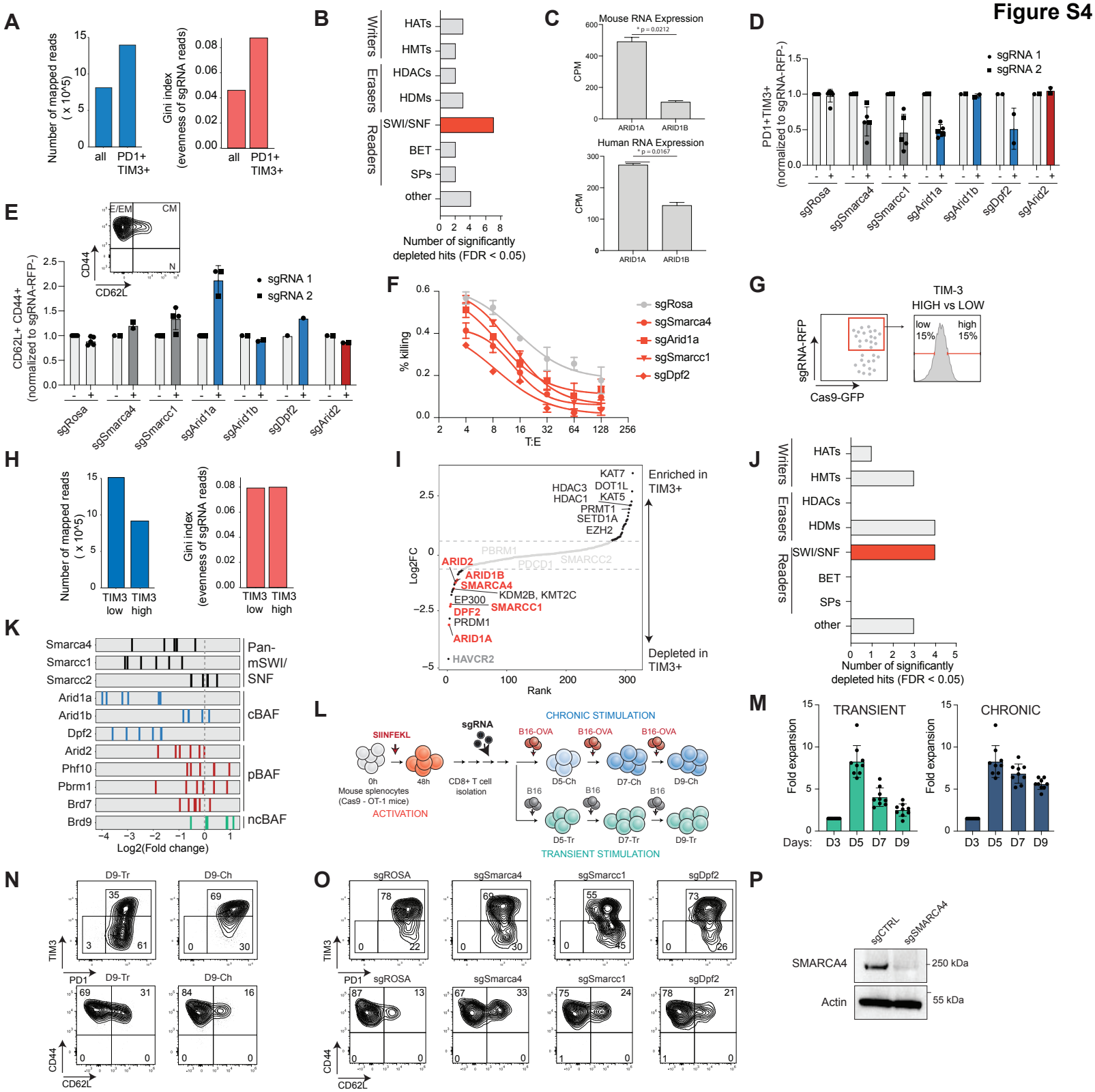

Figure S4. Contributions of mSWI/SNF (cBAF) complexes to T cell exhaustion in two independent CRISPR-Cas9-based screens in mouse CD8+ T cells, Related to Figure 4. A. Number of mapped reads (right) and Gini index representing the evenness of sgRNA reads (left) for the PD1+TIM3+ CRISPR screen. **B.** Number of significantly depleted hits (Log2FC < -1, FDR<0.05) within the indicated classed of chromatin writers, erasers or readers. **C.** Bar graph indicating the expression levels (RPKM) or ARID1A and ARID1B in mouse and human CD8+ T cells. **D.** Quantification of the PD1+TIM3+ population in cells infected with sgRNAs targeting the indicated genes, normalized to the sgRNA-negative population in the same culture, at Day9 of chronic stimulation. Different sgRNAs for the same gene are labeled with different shapes. Bar graphs represent mean ± SEM from 2-5 independent biological replicates. **E.** Quantification of the CD62L+ CD44+ population in cells infected with sgRNAs targeting the indicated genes, normalized to the sgRNA-negative population in the same culture, at Day9 of chronic stimulation. Different sgRNAs for the same gene are labeled with different shapes. Bar graphs represent mean ± SEM from 2-4 independent biological replicates. **F.** In vitro killing efficiency of B16-OVA cells by OT-1 T cells transduced with the indicated sgRNAs, at Day9 of chronic stimulation. B16-OVA cells and OT-1 T cells were co-incubated for 48 hours at the indicated Target-to-Effector (T:E) ratios. Means ± SEM from 4 technical replicates are shown. **G.** Sorting strategy for the TIM3 High vs Low screen using a custom sgRNA library of chromatin regulators. **H.** Number of mapped reads (right) and Gini index representing the evenness of sgRNA reads (left) for the TIM3 High vs Low CRISPR screen. **I.** Rank plot depicting Log2FC scores (average of n=6 guides) targeting all chromatin regulator genes and negative/positive controls. Depleted genes are highlighted in black; positive controls are highlighted in gray; mSWI/SNF complex genes are highlighted in orange. **J.** Number of significantly depleted hits (Log2FC < -1, FDR<0.05) within the indicated classed of chromatin writers, erasers or readers in the TIM3 High vs Low CRISPR screen. **K.** Log2FC values for n=6 independent guides in the TIM3 High vs Low CRISPR screen. **L.** Schematic for stimulation of mouse OT-1 CD8+ T cells based on co-culture with B16 or B16-OVA cells to profile early activation, transient stimulation, and chronic stimulation/exhaustion states. **M.** Fold expansion for mouse OT-1 CD8+ T cells in the chronic or transient stimulation conditions across the Day 3, 5, 5, 9 time points. Bar graphs represent mean ± SEM from 9 independent mice. **N.** FACS-based profiling of PD1, TIM3, CD62L and CD44 at Day9 of transient or chronic stimulation in mouse OT-1 CD8+ T cell studies. **O.** FACS-based profiling of PD1, TIM3, CD62L and CD44 at Day9 of chronic stimulation in control and mSWI/SNF subunit gene KO conditions. **P.** Western blot analysis of SMARCA4 levels in sgCTRL or sgSMARCA4 human CD8+ T cells, profiled at Day 9 of the chronic stimulation protocol, compared to actin as loading control.

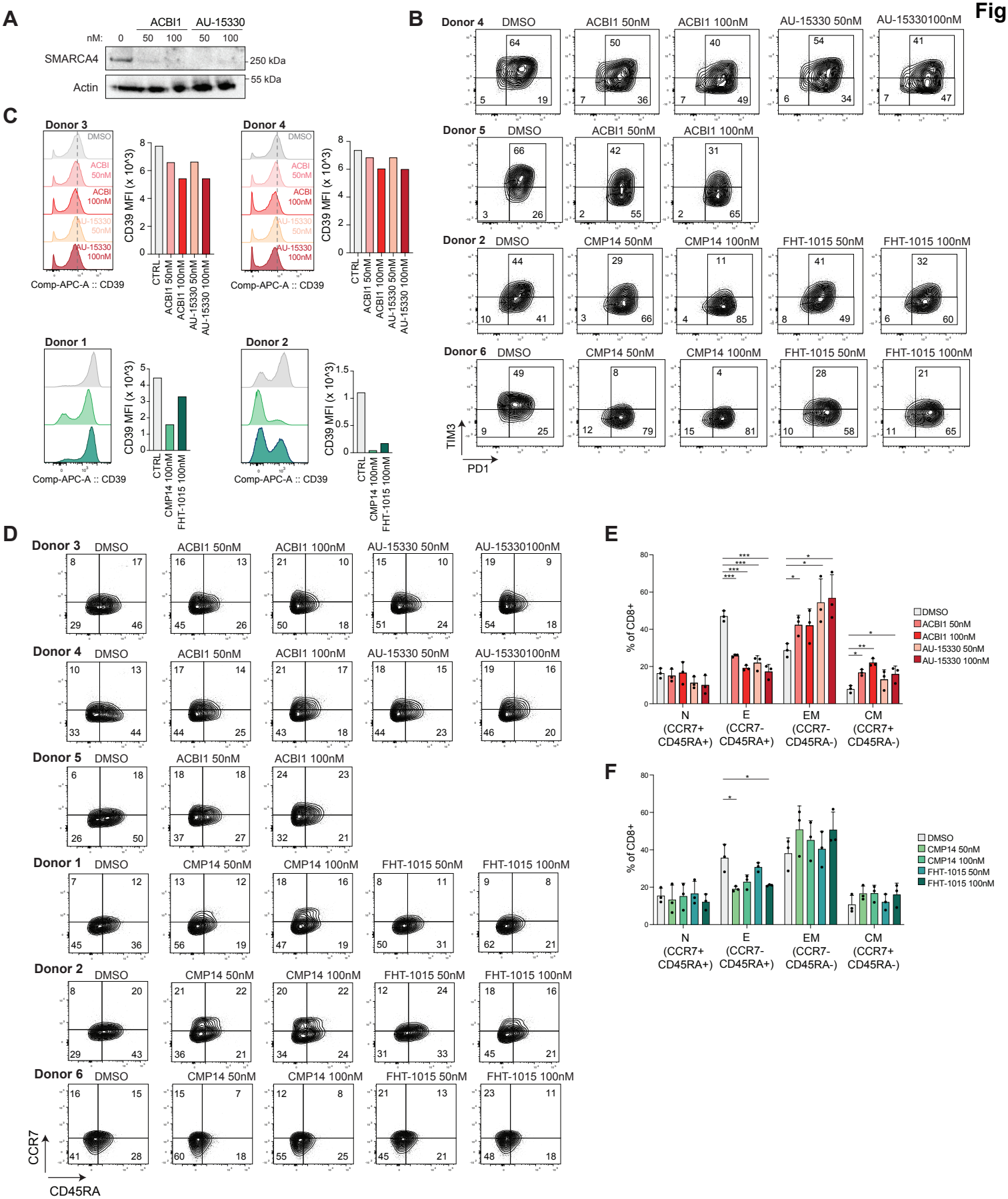

Figure S5. Evaluation of mSWI/SNF small molecule inhibitors and degraders in human T cells, Related to Figure 5. A. Western blot analysis of SMARCA4 levels in control, ACBI- or AU-15330- treated human CD8+ T cells at the indicated concentrations, profiled at Day 9 of the chronic stimulation protocol, compared to actin as loading control. **B.** FACS plots depicting PD1/TIM3 populations in CD8+ T cells from the indicated donors at Day 9 of chronic stimulation, treated with 50nm and 100nM of SMARCA4/2 degraders and inhibitors. **C.** FACS plots and associated MFI quantifications of CD39 surface levels in CD8+ T cells from the indicated donors at Day 9 of chronic stimulation, treated with 50nm and 100nM of SMARCA4/2 degraders (top) and inhibitors (bottom). **D.** FACS plots depicting CD45RA/CCR7 populations in CD8+ T cells from the indicated donors at Day 9 of chronic stimulation, treated with 50nm and 100nM of SMARCA4/2 degraders and inhibitors. **E.** Bar graph depicting % of CD8+ T cells in Naïve (N), Effector (E), Effector Memory (EM) and Central Memory (CM) populations based on CD45RA and CCR7 surface levels, in DMSO, ACBI1, and AU-15330 conditions. Error bars represent mean ± SEM of 3 independent CD8+ T cell donors. **F.** Bar graph depicting % of CD8+ T cells in Naïve (N), Effector (E), Effector Memory (EM) and Central Memory (CM) populations based on CD45RA and CCR7 surface levels, in DMSO, CMP14 and FHT1015 conditions. Error bars represent mean ± SEM of 3 independent CD8+ T cell donors. Error bars represent mean ± SEM of 3 technical replicates per donor. *p < 0.05, **p < 0.01, ***p < 0.001. ****p < 0.0001.

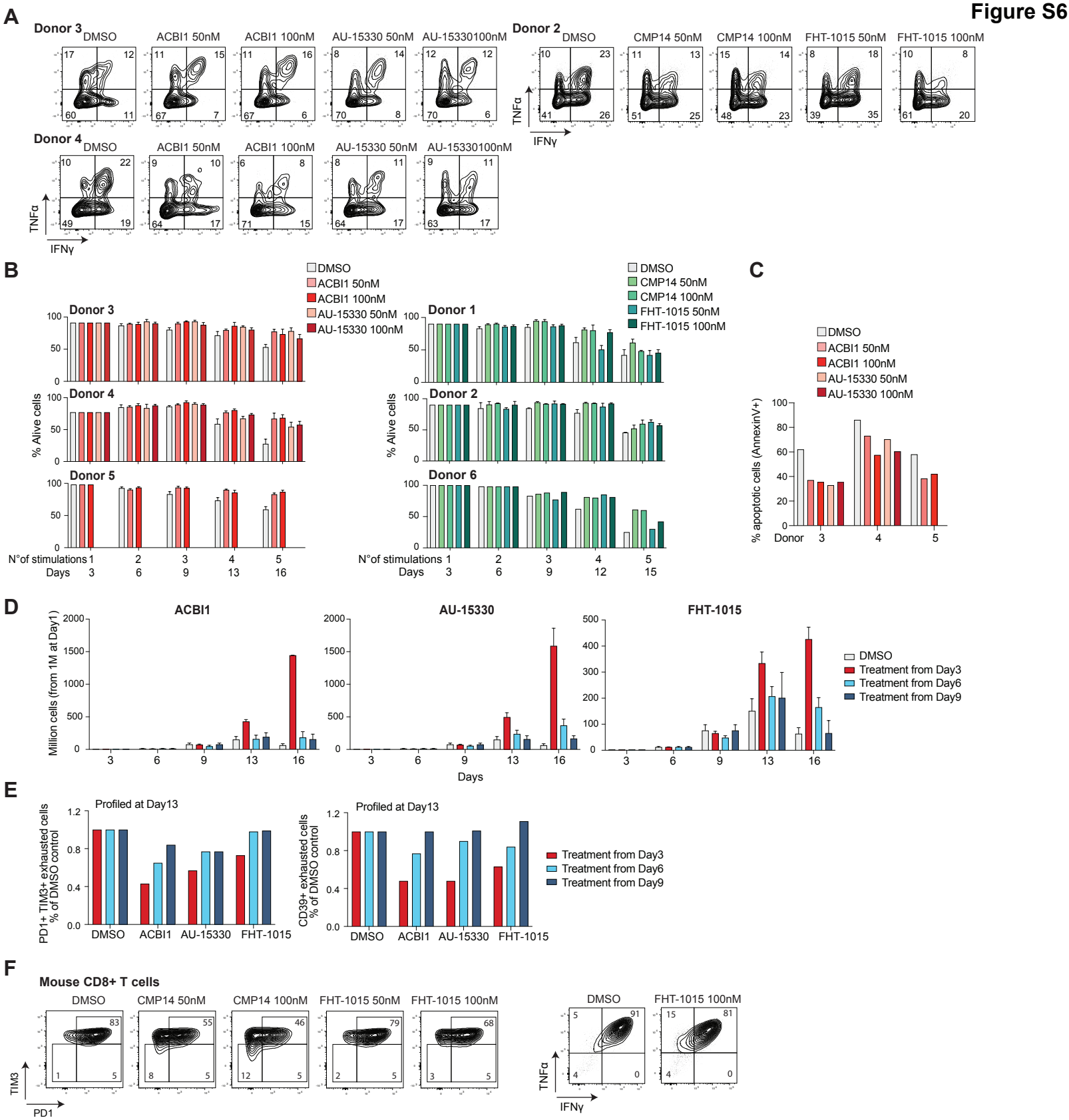

Figure S6. mSWI/SNF pharmacologic inhibition attenuates exhaustion of human and mouse T cells, Related to Figure 5,6. A. FACS plots depicting IFNγ/TNFα populations in CD8+ T cells from the indicated donors at Day 9 of chronic stimulation, treated with 50nm and 100nM of SMARCA4/2 degraders and inhibitors. **B.** Bar graphs depicting the percentage of alive cells at Days 3, 6, 9, 13 and 16 of chronic stimulation, for the indicated donors, treated with 50nm and 100nM of SMARCA4/2 degraders (left) and inhibitors (right). Error bars represent mean ± SEM of three technical replicates. **C.** Quantification of the percentage of apoptotic cells indicated by AnnexinV staining, at Day 16 of the chronic stimulation protocol, for the indicated donors treated with 50nm and 100nM of SMARCA4/2 degraders. **D.** Bar graphs depicting cell number upon treatment with ACBI1, AU-15330 or FHT-1015 (10^6 cells/10^ 6 cells at Day 0), initiated at the indicated time points, in one human CD8+ T cell donor. **E.** Quantification of the PD1+TIM3+ population in human CD8+ T cells upon treatment with ACBI1, AU-15330 or FHT-1015, initiated at the indicated time points. Data from one CD8+ T cell donor are represented. **F.** FACS plots depicting PD1/TIM3 (right) and IFNγ/TNFα (left) populations in mouse CD8+ T cells at Day 9 of chronic stimulation, treated with the indicated concentrations of SMARCA4/2 inhibitors.

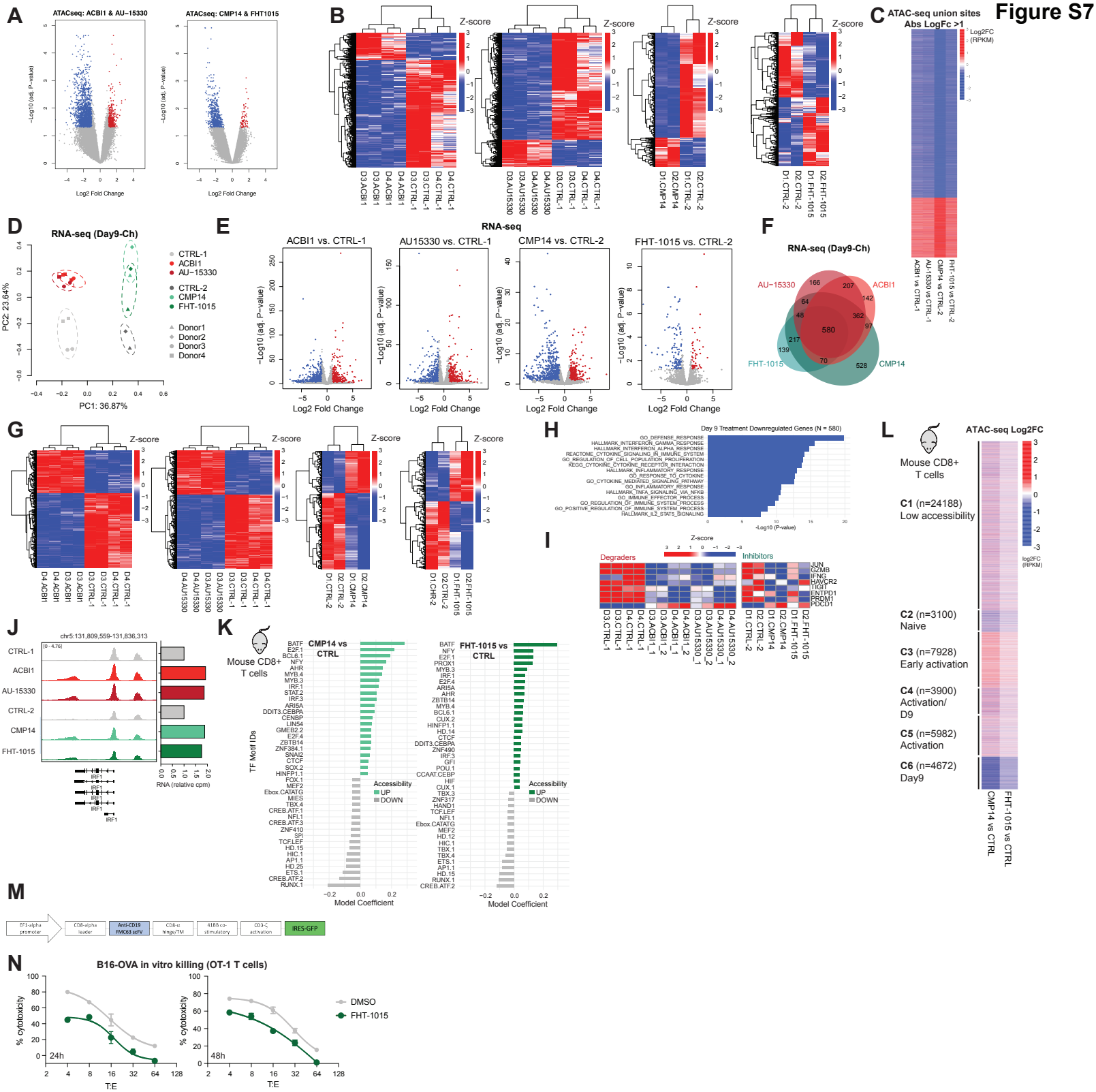

Figure S7. Chromatin accessibility, gene expression and T cell effector functional profiling in human and mouse T cells treated with mSWI/SNF inhibitors and degraders, Related to Figure 6,7. A. Volcano plots of changes in accessibility upon mSWI/SNF disruption (100nM); inhibitors and degraders are grouped. Significantly up-regulated and down-regulated genes (Abs Log2FC> 1, adjP< 0.05) are colored in red and blue, respectively. Differential accessibility was calculated from n=2 independent human CD8+ T cell donors. **B.** Hierarchical-clustered heatmap of ATAC-seq sites changes upon treatment with the indicated compounds (100nM). The top 5% most significant differentially accessible peaks are shown. **C.** K-means clustering (n=2) of ATAC-seq log2 fold changes upon treatment with the four inhibitors/degraders relative to DMSO control (averaged independent donors). **D.** Principal component analyses (PCA) of RNA-seq profiles of Control (CHR), and ACBI1, AU-15330, CMP14 or FHT-1015-treated human CD8+ T cells (100nM), at Day9. CHR.1 and CHR.2 are the controls for the ACBI1/AU-15330 and CMP14/FHT-1015 experiments, respectively. **E.** Volcano plots of changes in gene expression upon treatment with the indicated compounds (100nM). Significantly up-regulated and down-regulated genes (Abs Log2FC > 1, adjp< 0.05) are colored in red and blue, respectively. Differential expression was calculated from n=2 independent human CD8+ T cell donors. **F.** Venn diagram showing the overlap in down-regulated genes (LogFC <-1) upon treatment with ACBI1, AU-15330, CMP14 or FHT-1015 (100nM). **G.** Hierarchical-clustered heatmaps of gene expression changes upon treatment with the indicated compounds (100nM). The top 1000 differentially expressed genes are shown. **H.** Gene ontology analysis of the 580 down-regulated genes shared among treatment with ACBI1, AU-15330, CMP14 and FHT-1015. **I.** Z-scored heatmap reflecting the expression of selected genes following mSWI/SNF inhibitor or degrader treatments. **J.** Representative ATAC-seq tracks of untreated (CTRL) or treated T cells over the IRF1 locus with corresponding RNAseq gene expression levels. **K.** Top 40 coefficients of logistic regression models fitting motif counts across all sites to changes in accessibility upon treatment with CMP14 or FHT-1015 in mouse CD8+ T cells. **L.** Heatmap displaying ATAC-Seq log2 fold change values upon treatment with CMP14 or FHT-1015, with clusters from Fig. S3a indicated. **M.** Schematic of anti-CD19 CAR-T construct used for CAR-T cell studies. **N.** In vitro killing efficiency of B16-OVA cells by OT-1 T cells treated with FHT-1015 (100nM), at Day9 of chronic stimulation. B16-OVA cells and OT-1 T cells were co-incubated for 24 hours (left) or 48 hours (right) at the indicated Target-to-Effector (T:E) ratios. Means ± SEM from 4 technical replicates are shown.